PTPN23-dependent ESCRT machinery functions as a cell death checkpoint in restraining multiple cell death pathways

Dongyan Song[1,2], Yuxin Cen[1,2], Zhe Qian[1,2], Xiaoli S. Wu[1,3], Keith Rivera[1], Tse-Luen Wee[1], Osama E. Demerdash[1], Kenneth Chang[1], Darryl Pappin[1], Christopher R. Vakoc[1] and Nicholas K. Tonks[1]*

Supplementary Information

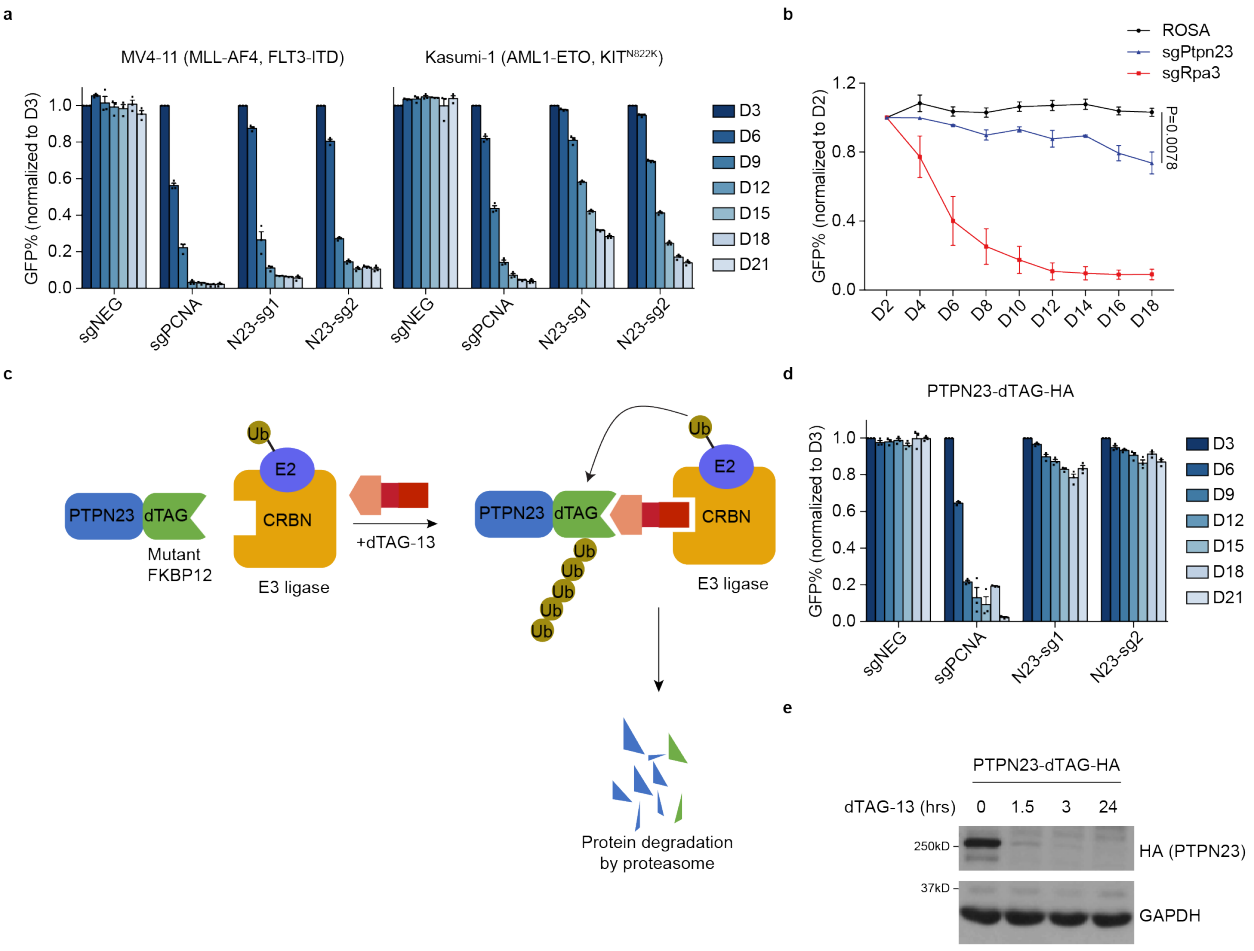

Supplementary Fig. 1. PTPN23 is required for AML cell survival. Related to Fig. 1. **a,** GFP competition growth assays of PTPN23 sgRNA KO in MV4-11 and Kasumi-1 human AML cells (n = 3 independent experiments). **b,** GFP competition growth assay of NIH 3T3 cells with guide RNAs targeting the mouse ROSA locus, Ptpn23, and Rpa3 (n = 3 independent experiments). Data are depicted as mean ± SEM. Statistical significance was determined using a two-tailed Wilcoxon matched-pairs signed rank test. **c,** Scheme depiction of the dTAG system. **d,** GFP competition growth assay of NOMO-1 cells stably expressing C-terminally fused dTAG to full-length PTPN23 construct (n = 3 independent experiments). **e,** Immunoblot showing the time course of PTPN23-dTAG-HA degradation upon dTAG-13 treatment (n = 3 independent experiments). Cell were treated with 100nM dTAG-13. Data are presented as mean ± SEM.

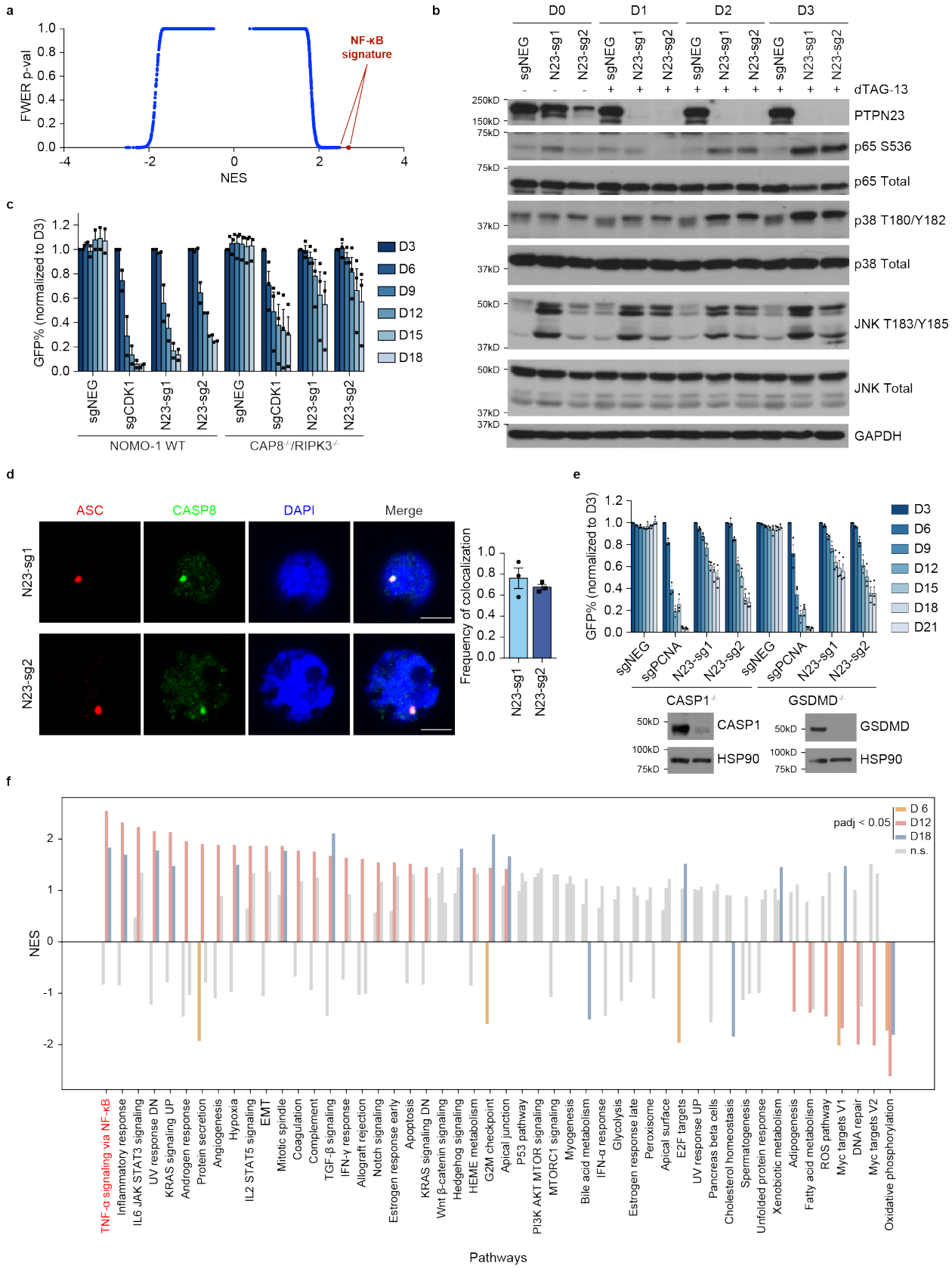
a
FWER p-val
NES
NF-κB signature
b
D0
D1
D2
D3
sgNEG
N23-sg1
N23-sg2
dTAG-13
PTPN23
p65 S536
p65 Total
p38 T180/Y182
p38 Total
JNK T183/Y185
JNK Total
GAPDH
c
GFP% (normalized to D3)
D3
D6
D9
D12
D15
D18
sgCDK1
NOMO-1 WT
CAP8-/-/RIPK3-/-
d
ASC
CASP8
DAPI
Merge
Frequency of colocalization
e
D21
sgPCNA
CASP1-/-
GSDMD-/-
CASP1
GSDMD
HSP90
f
padj < 0.05
n.s.
NES
Pathways
TNF-α signaling via NF-κB
Inflammatory response
IL6 JAK STAT3 signaling
UV response DN
KRAS signaling UP
Androgen response
Protein secretion
Angiogenesis
Hypoxia
IL2 STAT5 signaling
EMT
Mitotic spindle
Coagulation
Complement
TGF-β signaling
IFN-γ response
Allograft rejection
Notch signaling
Estrogen response early
Apoptosis
KRAS signaling DN
Wnt β-catenin signaling
Hedgehog signaling
HEME metabolism
G2M checkpoint
Apical junction
P53 pathway
PI3K AKT MTOR signaling
MTORC1 signaling
Myogenesis
Bile acid metabolism
IFN-α response
Glycolysis
Estrogen response late
Peroxisome
Apical surface
E2F targets
UV response UP
Pancreas beta cells
Cholesterol homeostasis
Spermatogenesis
Unfolded protein response
Xenobiotic metabolism
Adipogenesis
Fatty acid metabolism
ROS pathway
Myc targets V1
DNA repair
Myc targets V2
Oxidative phosphorylation

Supplementary Fig. 2. PTPN23 depletion led to activation of NF-κB signaling. Related to Fig. 2.

a, Plot of normalized enrichment score (NES) against family-wise error rate (FWER) *p*-value generated from GSEA analysis of 3,591 gene sets. **b,** Immunoblots of p65, p38 and JNK in PTPN23-dTAG NOMO-1 cells treated with 200 nM dTAG-13 for 0-3 days. (n = 3 independent experiments) **c,** GFP competition growth assay performed in the WT or CASP8/RIPK3 double knockout NOMO-1 cells (n = 2 independent experiments for NOMO-1 WT cells and n = 3 independent experiments for $CASP8^{-/-}RIPK3^{-/-}$ NOMO-1 cells). **d,** Left panel, representative images of immunofluorescence microscopy of ASC and CASP8 in PTPN23-dTAG NOMO-1 cells. Scale bar: 5 μm. Right panel, frequency of CASP8 and ASC colocalization upon PTPN23 sgRNA infection (n = 3 independent experiments, and 10 – 14 fields were captured in each experiment.). Data are presented as mean ± SEM. **e,** Top, GFP competition growth assays conducted using CASP1 or GSDMD knockout cells (n = 3 independent experiments). Data are presented as mean ± SEM. Bottom, Immunoblots of CASP1 and GSDMD in NOMO-1 cells utilized in the top experiments. **f,** Gene set enrichment analysis (GSEA) for 50 Hallmark Gene Sets comparing PTPN23 WT and KO samples across multiple time points post-infection. CASP8/RIPK3/GSDMD triple knockout NOMO-1 cells were infected with sgNEG, N23-sg1 or N23-sg2 lentivirus. RNA-seq data were derived from two biological replicates per sample, contrasting PTPN23 WT and KO samples at Day 6, 12, and 18 post-infection.

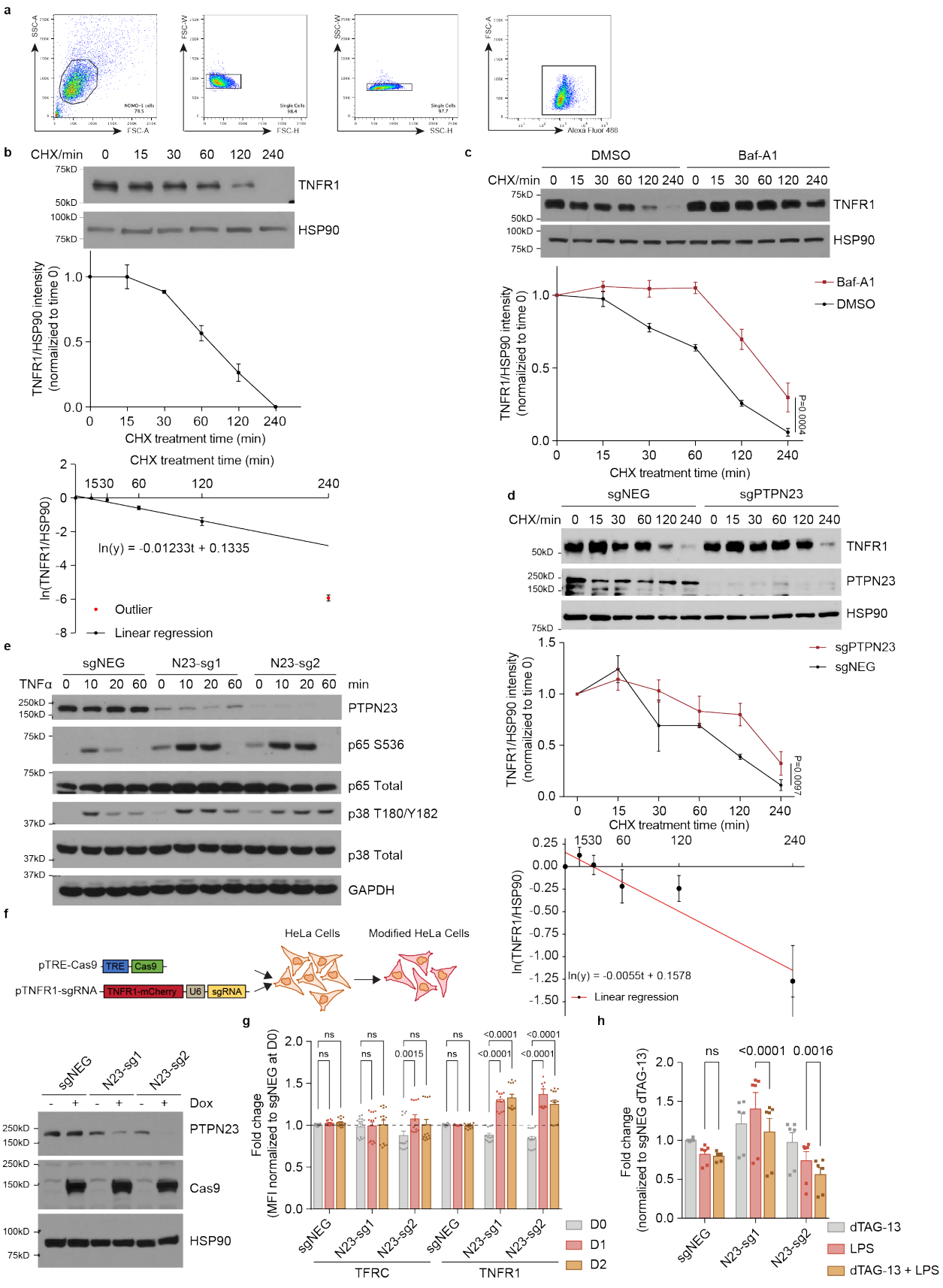
a
SSC-A
FSC-A
FSC-W
FSC-H
SSC-W
SSC-H
FSC-A
Alexa Fluor 488
b
CHX/min 0 15 30 60 120 240
75kD
TNFR1
50kD
100kD
HSP90
75kD
TNFR1/HSP90 intensity (normalized to time 0)
CHX treatment time (min)
ln(TNFR1/HSP90)
ln(y) = -0.01233t + 0.1335
Outlier
Linear regression
c
DMSO
Baf-A1
CHX/min 0 15 30 60 120 240 0 15 30 60 120 240
TNFR1
HSP90
Baf-A1
DMSO
P=0.0004
d
sgNEG
sgPTPN23
TNFR1
PTPN23
HSP90
sgPTPN23
sgNEG
P=0.0097
ln(TNFR1/HSP90)
ln(y) = -0.0055t + 0.1578
e
sgNEG
N23-sg1
N23-sg2
TNFα 0 10 20 60 0 10 20 60 0 10 20 60 min
250kD
150kD
PTPN23
75kD
p65 S536
p65 Total
37kD
p38 T180/Y182
p38 Total
GAPDH
f
HeLa Cells
Modified HeLa Cells
pTRE-Cas9
TRE
Cas9
pTNFR1-sgRNA
TNFR1-mCherry
U6
sgRNA
sgNEG
N23-sg1
N23-sg2
Dox
PTPN23
Cas9
HSP90
g
Fold chage (MFI normalized to sgNEG at D0)
ns
0.0015
<0.0001
D0
D1
D2
TFRC
TNFR1
h
Fold change (normalized to sgNEG dTAG-13)
ns
<0.0001
0.0016
dTAG-13
LPS
dTAG-13 + LPS

Supplementary Fig. 3. Modulation of receptor regulation upon PTPN23 depletion. Related to Fig. 3.

a, Gating strategy for flow cytometric analysis used to quantify the expression levels of TNFR1, FAS, DR4, DR5, TLR4, and TFRC as presented in this manuscript. **b,** Top, immunoblots of endogenous TNFR1 following CHX treatment in NOMO-1 cells. Middle, quantification of TNFR1/HSP90 intensity, n=3 independent experiments. Bottom, natural logarithm-transformed TNFR1/HSP90 ratio against time, utilized for calculating half-life ($t_{1/2}$). The $t_{1/2}$ equation: $t_{1/2} = (\ln(0.5) - 0.1335)/-0.01233$. The data point at 240 min was excluded due to intensity falling below the immunoblotting detection level. **c,** Top, immunoblots of TNFR1 following CHX treatment. NOMO-1 cells were pretreated with DMSO or 250 nM Baf-A1 for 2 hours. Bottom, quantification of TNFR1/HSP90 intensity, n = 3 independent experiments. **d,** Top, immunoblots of endogenous TNFR1 following CHX treatment in PTPN23-dTAG NOMO-1 cells. Prior to CHX treatment, the cells were treated with 200 nM dTAG-13 for 24 hours. Middle, quantification of TNFR1/HSP90 intensity, based on three independent experiments. Bottom, natural logarithm-transformed TNFR1/HSP90 ratio against time. The $t_{1/2}$ equation: $t_{1/2} = (\ln(0.5) - 0.1578)/-0.0055 = 154.7 \pm 25.4$ minutes. **e,** Immunoblots of p65 and p38 in NOMO-1 cells transfected with negative control sgRNA or two PTPN23 sgRNAs. Cells were stimulated with 20 ng/ml TNF-α for the indicated time at day 6 post-infection (n = 3 independent experiments). **f,** Top, schematic depiction of engineered HeLa cells. Bottom, immunoblots of PTPN23 in modified HeLa cells treated with 1 μg/ml doxycycline (Dox) or vehicle control for 5 days (n = 3 independent experiments). **g,** Fold changes of TFRC and TNFR1 measured by flow cytometry in PTPN23-dTAG NOMO-1 cells treated with 200 nM dTAG-13 over 0-2 days. The dataset comprises n = 13 samples across 3 independent experiments. **h,** Cytotoxicity of LPS in PTPN23-dTAG NOMO-1 cells. Cells were incubated with 1 μM dTAG-13 or 1 μg/ml LPS as indicated for 48 hours, and cell viability was measured using CTG assay (n = 6, 3 independent experiments). Data are presented as mean $\pm$ SEM. Statistical analysis for **b**, **c**, **d**, **g**, and **h** by two-way ANOVA, Tukey's multiple comparisons test.

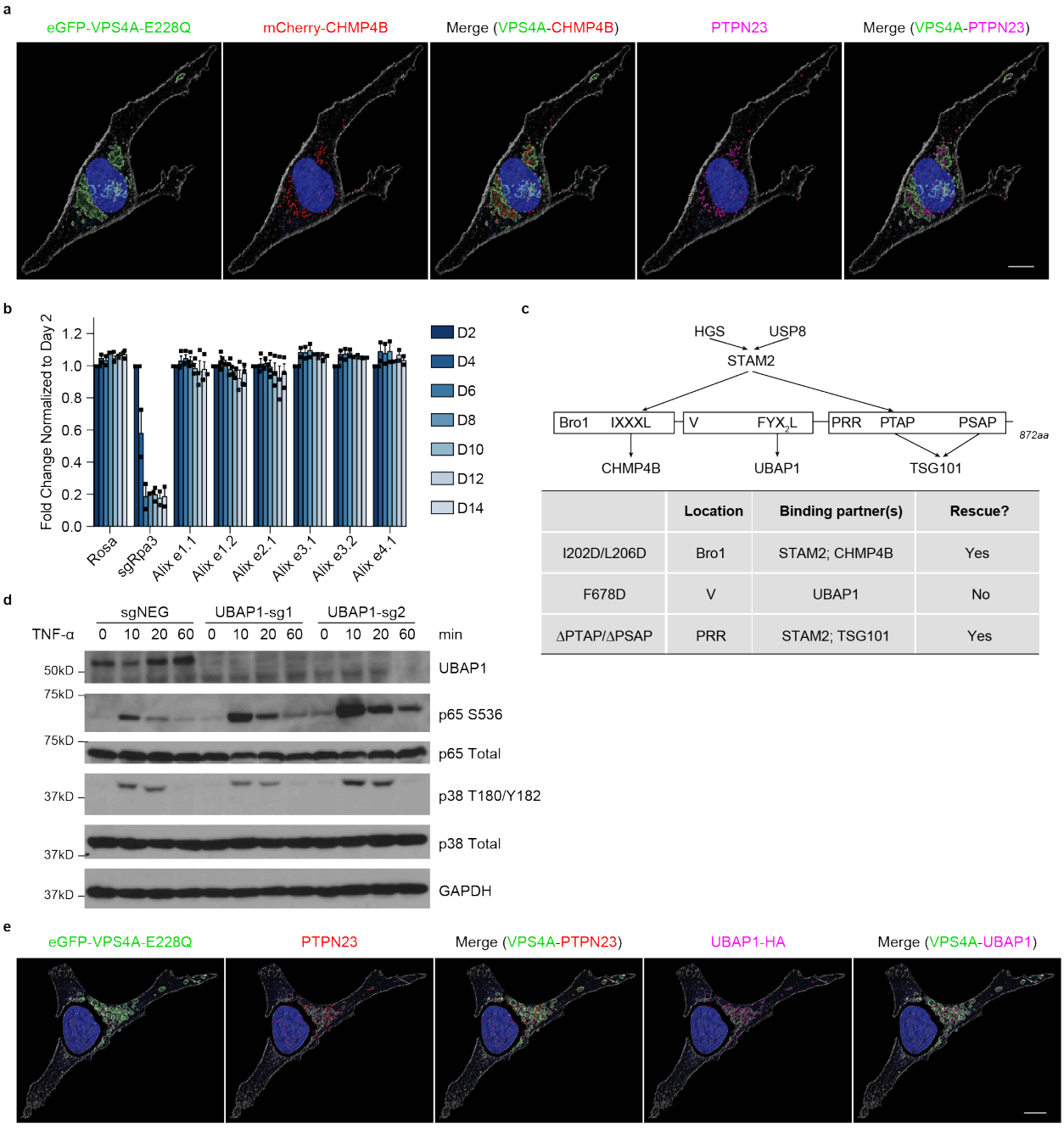

	Location	Binding partner(s)	Rescue?
I202D/L206D	Bro1	STAM2; CHMP4B	Yes
F678D	V	UBAP1	No
ΔPTAP/ΔPSAP	PRR	STAM2; TSG101	Yes

Supplementary Fig. 4. The essential role of PTPN23 was dependent on its V domain through interacting with UBAP1. Related to Fig. 4.

a, The 3D reconstructions of Fig. 4a showing the construction of eGFP-VPS4A-E228Q surfaces, mCherry-CHMP4B and PTPN23 spots. Scale bar: 10 μm. **b,** GFP competition growth assay of *Alix* knockout in RN2 cells (n = 2 independent experiments for Rosa,

sgRpa3, Alix e3.1, Alix3.2, and Alix e4.1; n = 3 independent experiments for Alix e1.1, Alix e1.2, and Alix e2.1). Data are presented as mean ± SEM. **c,** Top, summary of the ESCRT components binding to PTPN23 and the corresponding interaction motifs. Bottom, the ability of PTPN23 mutants to compensate *Ptpn23* knockout in RN2 cells. **d,** Immunoblotting analysis of p65 and p38 phosphorylation in response to UBAP1 depletion. NOMO-1 cells were stimulated with 20 ng/ml TNF-α for the indicated time at day 6 post sgRNA infection (n = 3 independent experiments). **e,** The 3D reconstructions of Fig. 4g showing the construction of eGFP-VPS4A-E228Q surfaces, PTPN23 and UBAP1-HA spots. Scale bar: 10 μm.

a

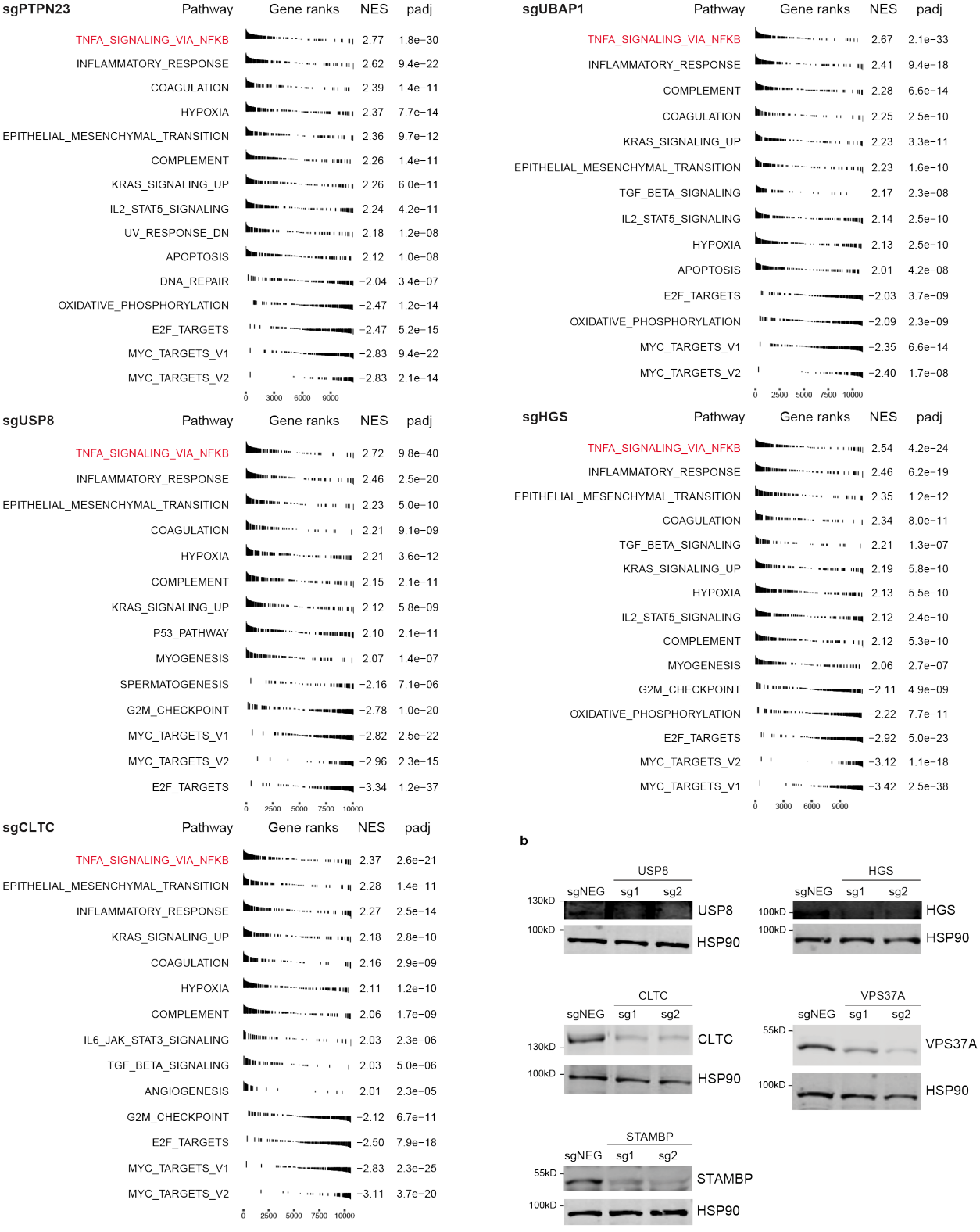
sgPTPN23
Pathway
Gene ranks
NES
padj
TNFA_SIGNALING_VIA_NFKB 2.77 1.8e−30
INFLAMMATORY_RESPONSE 2.62 9.4e−22
COAGULATION 2.39 1.4e−11
HYPOXIA 2.37 7.7e−14
EPITHELIAL_MESENCHYMAL_TRANSITION 2.36 9.7e−12
COMPLEMENT 2.26 1.4e−11
KRAS_SIGNALING_UP 2.26 6.0e−11
IL2_STAT5_SIGNALING 2.24 4.2e−11
UV_RESPONSE_DN 2.18 1.2e−08
APOPTOSIS 2.12 1.0e−08
DNA_REPAIR −2.04 3.4e−07
OXIDATIVE_PHOSPHORYLATION −2.47 1.2e−14
E2F_TARGETS −2.47 5.2e−15
MYC_TARGETS_V1 −2.83 9.4e−22
MYC_TARGETS_V2 −2.83 2.1e−14
0 3000 6000 9000
sgUSP8
Pathway
Gene ranks
NES
padj
TNFA_SIGNALING_VIA_NFKB 2.72 9.8e−40
INFLAMMATORY_RESPONSE 2.46 2.5e−20
EPITHELIAL_MESENCHYMAL_TRANSITION 2.23 5.0e−10
COAGULATION 2.21 9.1e−09
HYPOXIA 2.21 3.6e−12
COMPLEMENT 2.15 2.1e−11
KRAS_SIGNALING_UP 2.12 5.8e−09
P53_PATHWAY 2.10 2.1e−11
MYOGENESIS 2.07 1.4e−07
SPERMATOGENESIS −2.16 7.1e−06
G2M_CHECKPOINT −2.78 1.0e−20
MYC_TARGETS_V1 −2.82 2.5e−22
MYC_TARGETS_V2 −2.96 2.3e−15
E2F_TARGETS −3.34 1.2e−37
0 2500 5000 7500 10000
sgCLTC
Pathway
Gene ranks
NES
padj
TNFA_SIGNALING_VIA_NFKB 2.37 2.6e−21
EPITHELIAL_MESENCHYMAL_TRANSITION 2.28 1.4e−11
INFLAMMATORY_RESPONSE 2.27 2.5e−14
KRAS_SIGNALING_UP 2.18 2.8e−10
COAGULATION 2.16 2.9e−09
HYPOXIA 2.11 1.2e−10
COMPLEMENT 2.06 1.7e−09
IL6_JAK_STAT3_SIGNALING 2.03 2.3e−06
TGF_BETA_SIGNALING 2.03 5.0e−06
ANGIOGENESIS 2.01 2.3e−05
G2M_CHECKPOINT −2.12 6.7e−11
E2F_TARGETS −2.50 7.9e−18
MYC_TARGETS_V1 −2.83 2.3e−25
MYC_TARGETS_V2 −3.11 3.7e−20
0 2500 5000 7500 10000
sgUBAP1
Pathway
Gene ranks
NES
padj
TNFA_SIGNALING_VIA_NFKB 2.67 2.1e−33
INFLAMMATORY_RESPONSE 2.41 9.4e−18
COMPLEMENT 2.28 6.6e−14
COAGULATION 2.25 2.5e−10
KRAS_SIGNALING_UP 2.23 3.3e−11
EPITHELIAL_MESENCHYMAL_TRANSITION 2.23 1.6e−10
TGF_BETA_SIGNALING 2.17 2.3e−08
IL2_STAT5_SIGNALING 2.14 2.5e−10
HYPOXIA 2.13 2.5e−10
APOPTOSIS 2.01 4.2e−08
E2F_TARGETS −2.03 3.7e−09
OXIDATIVE_PHOSPHORYLATION −2.09 2.3e−09
MYC_TARGETS_V1 −2.35 6.6e−14
MYC_TARGETS_V2 −2.40 1.7e−08
0 2500 5000 7500 10000
sgHGS
Pathway
Gene ranks
NES
padj
TNFA_SIGNALING_VIA_NFKB 2.54 4.2e−24
INFLAMMATORY_RESPONSE 2.46 6.2e−19
EPITHELIAL_MESENCHYMAL_TRANSITION 2.35 1.2e−12
COAGULATION 2.34 8.0e−11
TGF_BETA_SIGNALING 2.21 1.3e−07
KRAS_SIGNALING_UP 2.19 5.8e−10
HYPOXIA 2.13 5.5e−10
IL2_STAT5_SIGNALING 2.12 2.4e−10
COMPLEMENT 2.12 5.3e−10
MYOGENESIS 2.06 2.7e−07
G2M_CHECKPOINT −2.11 4.9e−09
OXIDATIVE_PHOSPHORYLATION −2.22 7.7e−11
E2F_TARGETS −2.92 5.0e−23
MYC_TARGETS_V2 −3.12 1.1e−18
MYC_TARGETS_V1 −3.42 2.5e−38
0 3000 6000 9000

b

USP8
sgNEG sg1 sg2
130kD
100kD
USP8
HSP90
HGS
sgNEG sg1 sg2
100kD
100kD
HGS
HSP90
CLTC
sgNEG sg1 sg2
130kD
100kD
CLTC
HSP90
VPS37A
sgNEG sg1 sg2
55kD
100kD
VPS37A
HSP90
STAMBP
sgNEG sg1 sg2
55kD
100kD
STAMBP
HSP90

Supplementary Fig. 5. GSEA pathway enrichment and immunoblot analysis of PTPN23 and its co-dependent gene knockouts. Related to Fig. 5.

a. Enrichment plots for pathways with NES > 2 or < -2 from GSEA Hallmark analysis in RNA-seq comparing PTPN23 or its co-dependent gene knockouts to negative controls. **b.** Immunoblotting analysis of NOMO-1 cells infected with sgNEG or sgRNAs targeting the indicated genes (n = 3 independent experiments). Cells were harvested 5 days post-infection.

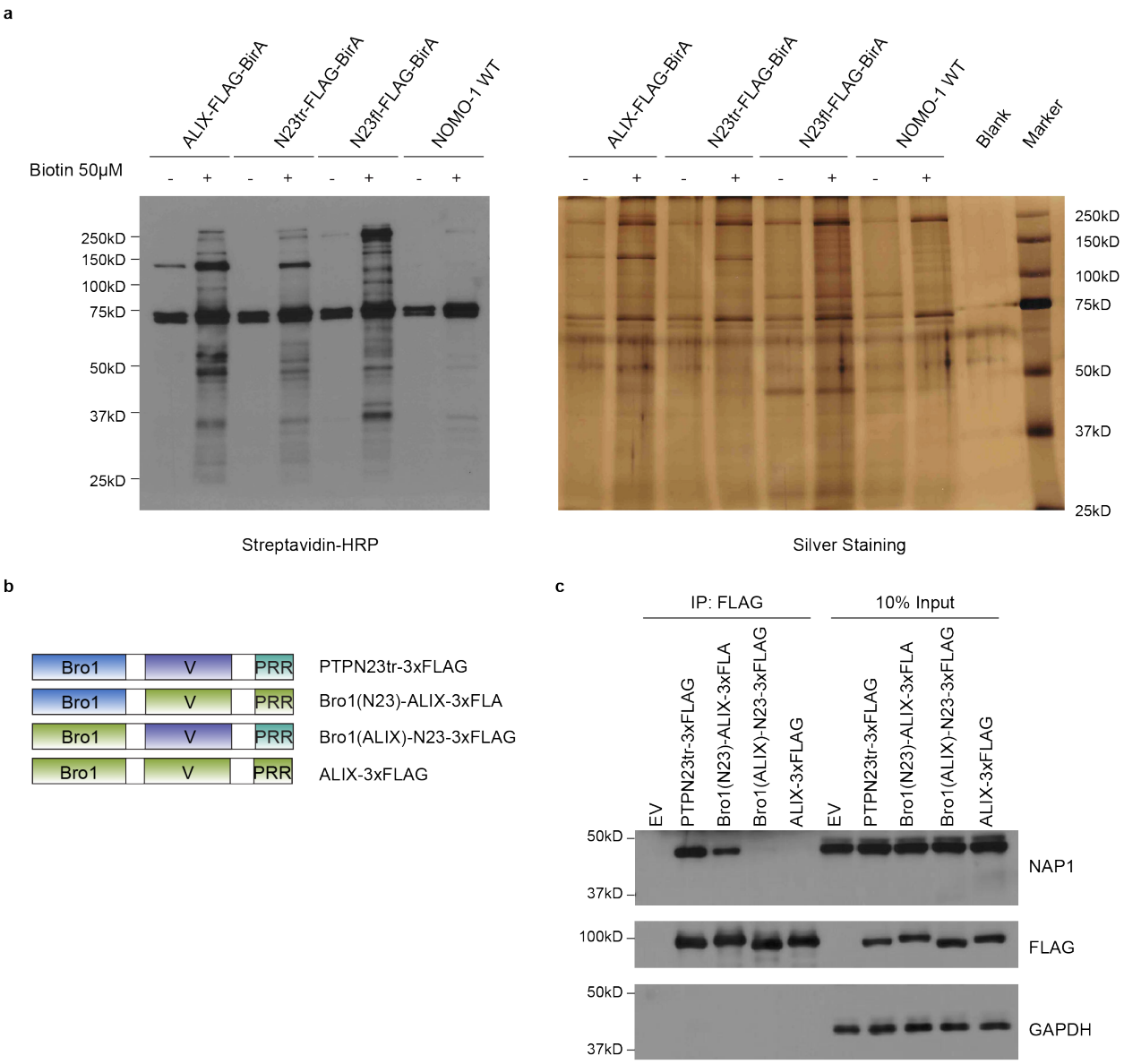

Supplementary Fig. 6. The Bro1 domain of PTPN23 binds to NAP1. Related to Fig. 6.

a, Representative blots to examine the quality of samples prior to MS analysis (n = 3 independent experiments). The left panel shows immunoblot results, and the right panel displays silver staining. **b,** Schematic representation of PTPN23tr, ALIX and chimeric proteins. **c,** Immunoprecipitation assay of endogenous NAP1 and overexpressed PTPN23tr, ALIX or PTPN23/ALIX chimeras in HEK 293T cells (n = 3 independent experiments). Indicated plasmids were transiently transfected into HEK 293T cells, and cells were harvested 48 hours post-transfection.

a

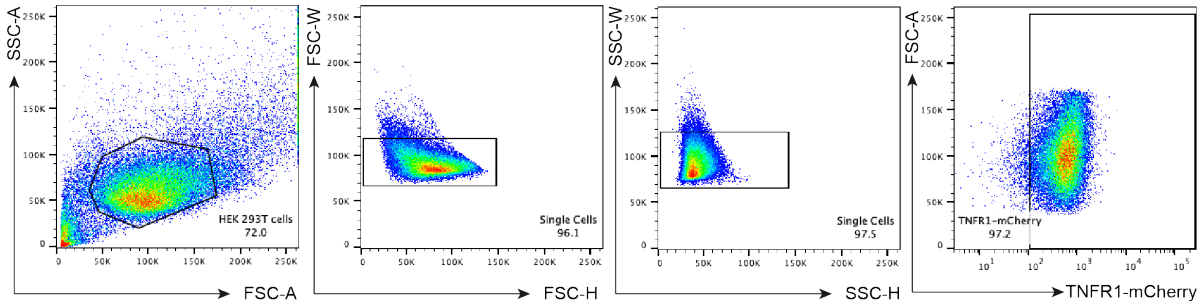
SSC-A
FSC-A
HEK 293T cells
72.0
FSC-W
FSC-H
Single Cells
96.1
SSC-W
SSC-H
Single Cells
97.5
FSC-A
TNFR1-mCherry
TNFR1-mCherry
97.2

b

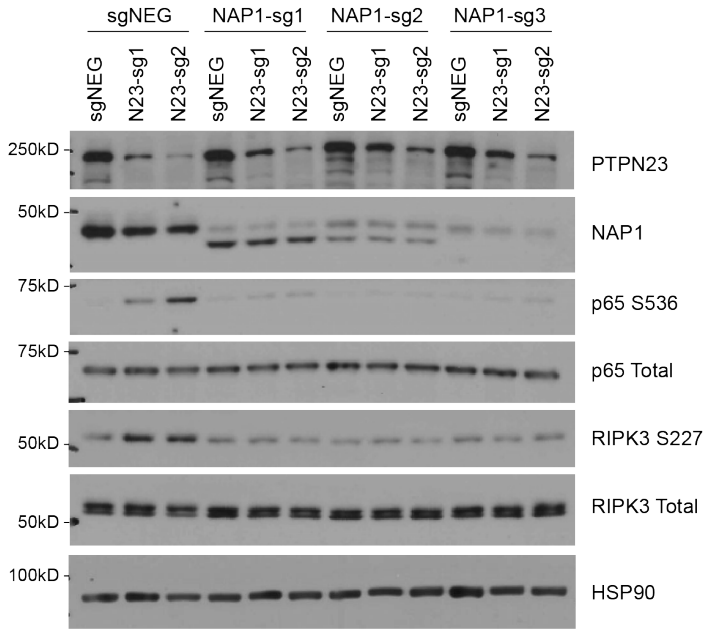
sgNEG
NAP1-sg1
NAP1-sg2
NAP1-sg3
sgNEG
N23-sg1
N23-sg2
250kD
PTPN23
50kD
NAP1
75kD
p65 S536
75kD
p65 Total
50kD
RIPK3 S227
50kD
RIPK3 Total
100kD
HSP90

c

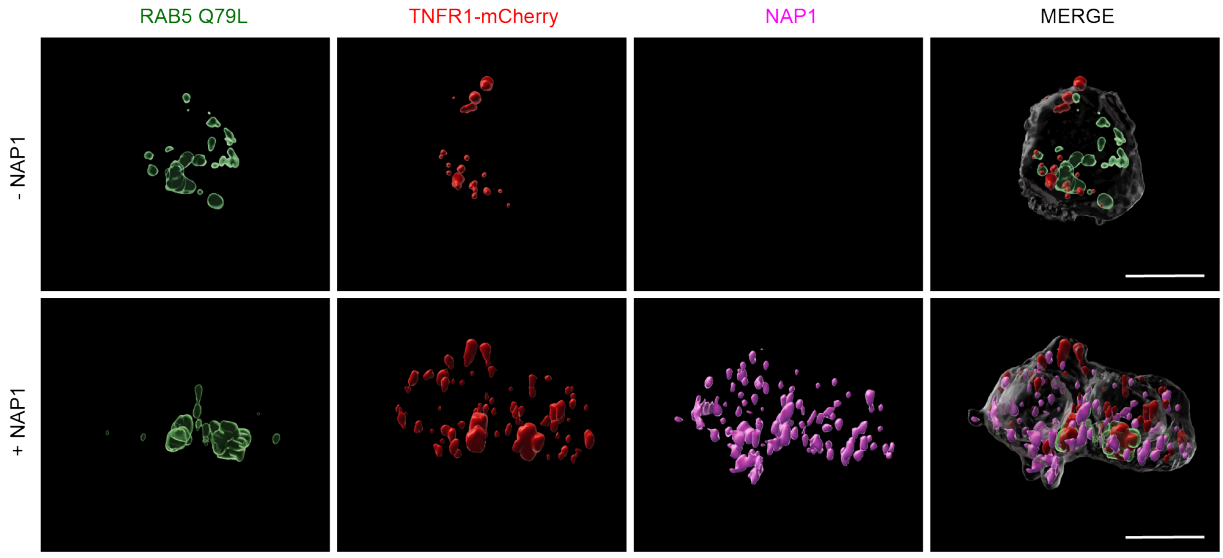
RAB5 Q79L
TNFR1-mCherry
NAP1
MERGE
- NAP1
+ NAP1

Supplementary Fig. 7. The impact of NAP1 on TNFR1 signaling regulation. Related to Fig. 7.

a, Gating strategy for flow cytometric analysis of mCherry-TNFR1 level. **b,** Immunoblots of p65 and RIPK3 examined upon PTPN23 depletion in the WT or NAP1-knockout NOMO-1 cells. Following infection with negative control or two PTPN23 sgRNAs, cells were harvested 6 days post-infection, with subsequent examination of p65 and RIPK3 phosphorylation status (n = 3 independent experiments). **c,** The 3D rendered images of Fig. 7e. Scale bar: 10 μm.